BBA - Molecular Basis of Disease 1863 (2017) 1492–1499

Contents lists available at ScienceDirect

BBA - Molecular Basis of Disease

journal homepage: www.elsevier.com/locate/bbadis

# MDH2 is an RNA binding protein involved in downregulation of sodium channel *Scn1a* expression under seizure condition

Yong-Hong Chen[1], Shu-Jing Liu[1], Mei-Mei Gao, Tao Zeng, Guo-Wang Lin, Na-Na Tan, Hui-Ling Tang, Ping Lu, Tao Su, Wei-Wen Sun, Long-Chang Xie, Yong-Hong Yi, Yue-Sheng Long*

*Institute of Neuroscience and Department of Neurology of the Second Affiliated Hospital of Guangzhou Medical University, Guangzhou 501260, China*
*Key Laboratory of Neurogenetics and Channelopathies of Guangdong Province and the Ministry of Education of China, Guangzhou 501260, China*

ARTICLE INFO

*Keywords:*
MDH2
*Scn1a*
Seizure
Posttranscriptional regulation
RNA binding protein

ABSTRACT

Voltage-gated sodium channel α-subunit type I ($Na_V1.1$, encoded by *SCN1A* gene) plays a critical role in the excitability of brain. Downregulation of *SCN1A* expression is associated with epilepsy, a common neurological disorder characterized by recurrent seizures. Here we reveal a novel role of malate dehydrogenase 2 (MDH2) in the posttranscriptional regulation of *SCN1A* expression under seizure condition. We identified that MDH2 was an RNA binding protein that could bind two of the four conserved regions in the 3′ UTRs of *SCN1A*. We further showed that knockdown of MDH2 or inactivation of MDH2 activity in HEK-293 cells increased the reporter gene expression through the 3′ UTR of *SCN1A*, and MDH2 overexpression decreased gene expression by affecting mRNA stability. In the hippocampus of seizure mice, the upregulation of MDH2 expression contributed to the decrease of the $Na_V1.1$ levels at posttranscriptional level. In addition, we showed that the $H_2O_2$ levels increased in the hippocampus of the seizure mice, and $H_2O_2$ could promote the binding of MDH2 to the binding sites of *Scn1a* gene, whereas β-mercaptoethanol decreased the binding capability, indicating an important effect of the seizure-induced oxidation on the MDH2-mediated downregulation of *Scn1a* expression. Taken together, these data suggest that MDH2, functioning as an RNA-binding protein, is involved in the posttranscriptional downregulation of *SCN1A* expression under seizure condition.

## 1. Introduction

The *SCN1A* gene, encoding voltage-gated sodium channel α-subunit type I ($Na_V1.1$), is one of the most pathogenic genes for epilepsy, a group of neurological diseases characterized by recurrent seizures. To date, more than 1200 mutations in the *SCN1A* coding region have been identified to be associated with epilepsy, and about half of them results in loss of function of the protein $Na_V1.1$ [1,2]. Additionally, mutations in the *SCN1A* untranslated region or promoter region have also been identified from epileptic patients [3–5]. Furthermore, *Scn1a*$^{+/-}$ mice display epileptic seizures [6]. These reports suggest that the down-regulation of *SCN1A* expression is associated with epilepsy.

Posttranscriptional regulation is an important process of control gene expression at the RNA level, and RNA binding proteins (RBPs) play an important role in this process by controlling alternative splicing, nuclear export, cytoplasmic distribution, degradation and ultimately translation [7,8]. RBPs achieve these events *via* binding the RNA recognition motifs on the mRNA transcripts, which typically locate within the 3′ untranslated region (3′ UTR) of the transcript [9–11]. It has been reported that there are a number of cytoplasmic proteins potentially functioning as RBPs, but their roles in posttranslational regulation remain to be elucidated [12]. Therefore, identification of new RBPs and their targets should be helpful for understanding the regulatory mechanism of gene expression at posttranscriptional level and its role in the pathogenesis of human diseases [10,13]. It is known that numerous metabolic enzymes have an RNA-binding activity that may play roles in metabolism-driven post-translational modifications and be associated neurological diseases [14–17]. Malate dehydrogenase 2 (MDH2), a metabolic enzyme to participate in the citric acid cycle by catalyzing the interconversion of malate to oxaloacetate, may act as an RNA-binding protein in regulating the mRNA process [12]. However, to our knowledge, there is no experimental evidence to demonstrate that MDH2 is involved in posttranscriptional regulation.

In this study, we report for the first time that the MDH2 is an RNA-binding protein that negatively regulates sodium channel *SCN1A* gene expression by binding to the conserved regions of 3′ UTR. We further

* Corresponding author at: Institute of Neuroscience and the Second Affiliated Hospital of Guangzhou Medical University, 250 Changang East Road, Guangzhou 510260, China.
*E-mail address:* longyuesheng@gzhmu.edu.cn (Y.-S. Long).
[1] These authors contributed equally to this work.

http://dx.doi.org/10.1016/j.bbadis.2017.04.018
Received 22 January 2017; Received in revised form 31 March 2017; Accepted 18 April 2017
Available online 19 April 2017

show that, in the hippocampus of seizure mice, *Scn1a* expression is downregulated by MDH2 under an oxidation condition, suggesting a relationship between MDH2 and epileptogenesis.

## 2. Materials and methods

### 2.1. Conservation analysis

The *SCN1A* 3′ UTR sequences of *Homo sapiens* (GenBank Accession No: NM_001165963) and *Mus musculus* (NM_018733), and the *SCN3A* 3′ UTR sequences of *Homo sapiens* (NM_006922) and *Mus musculus* (NM_018732), were aligned with the vector NTI (Informax). The conserved regions (CSs) were identified according to our previous descriptions [15].

### 2.2. Luciferase constructs and DNA constructs

*SCN1A* 3′ UTR and *SCN3A* 3′ UTR luciferase constructs were generated as our previous descriptions [15]. To generate MDH2 overexpression construct pCMV-MDH2, the *Mdh2* ORF was amplified from the construct pcDNA3.1-3xFlag-MDH2 purchased from (YouBao Biotechnology), and were then cloned into the *Nhe* I-*Sal* I site of the pCMV vector (Invitrogen). These constructs were confirmed by sequencing. For knockdown of MDH2, MDH2-specific small hairpin RNA (shRNA) plasmid and control shRNA plasmid were purchased from GenePharma Co., Ltd (Shanghai, China).

### 2.3. Cell culture, drug treatment and transfection

Human embryonic kidney 293 (HEK-293) cells and mouse neuroblastoma N1E-115 cells purchased from ATCC were cultured in Dulbecco's Modified Eagle's Medium (DMEM, Gibco) supplemented with 10% fetal bovine serum (Gibco) and antibiotics penicillin and streptomycin at a final concentration of 100 μg/ml. The cells were incubated at 37 °C under 5% $CO_2$. Before treatment with drugs, the cells were seeded in 6-well plates (3.5 $cm^2$) with 3.5 × $10^5$ cells per well and incubated overnight. The cells were then respectively treated with MDH2 inhibitor (K252C, Santa Cruz Biotech) at a final concentration of 10 μM and 20 μM. For MDH2 knockdown, 5 μg of MDH2-specific shRNA constructs or negative control shRNA constructs were transfected into HEK-293 cells using TurboFect Transfection Reagent (Thermo). After 72-h transfection, the cells were harvested for further analyses. For MDH2 overexpression, 5 μg of pCMV-MDH2 constructs or negative control constructs pCMV-null were transfected into the cells. After 48-h transfection, the cells were harvested for further analyses.

### 2.4. Luciferase assay

The cells were incubated at 37 °C under 5% $CO_2$. Before transfection, the HEK-293 cells were plated at 1 × $10^5$ cells per well in 96-well plates and the medium was changed to DMEM without FBS or the medium with K252C. In each well, the cells were transfected with 200 ng of the tested constructs using TurboFect Transfection Reagent (Thermo). The activities of Renilla luciferase and firefly luciferase were determined using the Dual-Luciferase Reporter Assay System (Promega). Luminescence was detected by a GloMax 20/20 Luminometer (Promega) according to the manufacturer's instructions and our previous descriptions [18,19]. Three technical repeats were performed for each transfection.

### 2.5. Mice and seizure induction

Kunming mice (closed strain, derived from Swiss mice) were obtained from Medical Experimental Animal Center of Guangdong Province (Foshan, China) and were bred at The Experimental Animal Center of Guangzhou Medical University. Only male mice and aged 2 weeks were used for the studies. This study was approved by the Ethical Committee for the use of experimental animals of Guangzhou Medical University. Total 40 mice (2 weeks old, about 12 g) were divided into normal and seizure groups (20 mice for each group). Evoked seizures were induced by a single intraperitoneal injection of kainic acid (KA; 20 mg/kg; Sigma-Aldrich) dissolved in saline. After KA treatment, the behavior of each mouse was observed for at least 2 h according to a previous report and our previous studies [20–22]. The seizure degree was evaluated according to the Racine scale, and the mice with tonic–clonic convulsions at level 5 were considered as seizure group. The control mice were injected with saline without KA at the same time. Two weeks later, 5 seizure mice and 5 control mice were used for further analyses.

### 2.6. RNA extraction and qRT-PCR

Total RNA samples were isolated from mouse hippocampus using PureLink® RNA Mini Kit (Thermo Scientific). The cDNAs were synthesized from the DNase-treated total RNA (1 μg) using ReverTra Ace qPCR RT Master Mix with gDNA Remover (TOYOBO) according to the manufacturer's protocol. The primers for qRT-PCR were to mouse *Scn1a* (5′-AACAGCCTGTCATTGAACCAGAAG-3′ and 5′-TTTGTCAGCATACTCCAGCATGG-3′), *Mdh2* (5′-TTCAACACCAACGCTACCATTGTG-3′ and 5′-GTGTTCGCTCTGACGATG TCAAGG-3′), *β-actin* (5′-TGGTCGTCGACAACGGCTC-3′ and 5′-CCATGTCGTCCCAGTT GGTAAC-3′) and *Tublin* (5′-CTTCGGGCAGATCTTCAGAC-3′ and 5′-CAGTCGA CATTGTAGGTGTG-3′). Real-time qPCR was performed using Thunderbird SYBR Q-PCR Mix (Toyobo) and Rotor-Gene™ Q instrument (Qiagen) according to the manufacturer's protocols. All of the cDNA samples were diluted to 200 ng for qPCR. The level of house-keeping genes *β-actin* was used as endogenous controls for normalization according to a previous description [23]. For mouse model, 3 technical replicates were performed with the RNA sample from each mouse.

### 2.7. mRNA stability analysis

The mRNA stability analysis was performed according to our previous descriptions [15]. Briefly, the half-lives of the reporter genes *hRluc* and *hluc* + mRNAs determined in HEK-293 cells or *Scn1a* and *Tublin* mRNAs in N1E-115 cells treated with actinomycin D (Invitrogen). The HEK-293 cells were co-transfected with luciferase constructs and MDH2-overexpression constructs or the N1E-115 cells were transfected MDH2-overexpression constructs for 48 h, following with addition of actinomycin D (10 μg/ml) to block gene transcription. After addition of actinomycin D, the cells were harvested at 0, 3 and 6 h, respectively. The levels of *hRluc* mRNA and *hluc* + mRNA or *Scn1a* and *Tublin* mRNAs at each time point were quantified by qRT-PCR as described above. Three technical replicates were performed with RNA sample from three independent transfections.

### 2.8. Western blot analysis

Cytoplasmic proteins from tissues or cells were extracted using reagent of NE-PER™ Nuclear and Cytoplasmic Extraction Reagents (Thermo Scientific) according to the manufacturer's instructions. Protein samples were quantified using BCA method. Protein fractions were then transferred to polyvinylidene difluoride (PVDF) membranes. The membranes were then incubated with primary antibodies anti-MDH2 (1:8000, Abcam, Cat#: ab181857), anti-Nav1.1 (1:500, Abcam, Cat#: ab24820), and anti-β-tubulin (1:3000, Abcam, Cat#: ab6046) respectively. A horseradish peroxidase-conjugated secondary antibody was added to the reaction and the bands were visualized using Supersignal West Pico Chemiluminescence (Pierce) and the bands were quantified using Photoshop CS software. Three biological replicates were performed for all the experiments.

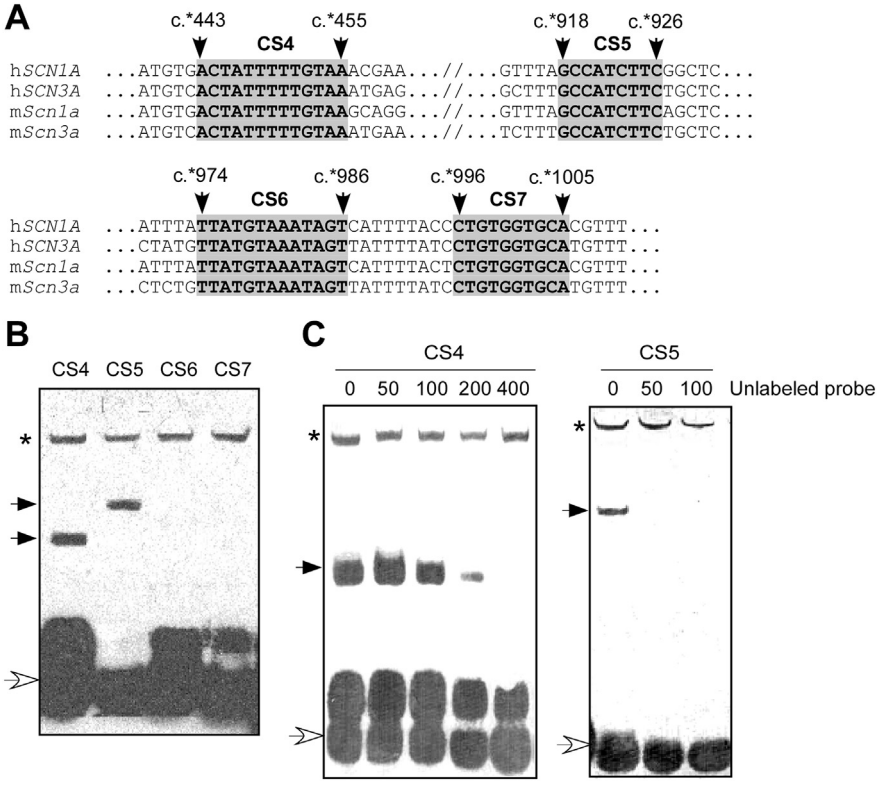


**Fig. 1. Binding of cytoplasmic extracts to the conserved regions on the *SCN1A* 3′ UTR.** (**A**) Conservation analyses of the 3′ UTRs of human and mouse *SCN1A* and *SCN3A*. The numbers and arrows represent the distance (nt) from the stop codon. The nucleotides displayed as gray background indicate the conserved regions named as CS4–7, respectively. (**B**) RNA-EMSA assays using the cytoplasmic extracts of HEK-293 cells and the biotin-labeled probes containing CS4–7, respectively. Shift probes and free probes were shown by solid arrow and hollow arrow, respectively. Unspecific bands were shown by asterisk. (**C**) Competition RNA-EMSA assays using the labeled probes and the unlabeled probes with a titration from 0 to 400 (for CS4) and from 0 to100 (for CS5), respectively. Shift probes and free probes were shown by solid arrow and hollow arrow, respectively. Unspecific bands were shown by asterisk.

### *2.9. RNA Electrophoretic Mobility Shift Assay (RNA-EMSA) and supershift assay*

RNA-EMSA using Lightshift Chemiluminescent EMSA kit (Thermo Scientific), which was conducted in a 20 μl complex containing 1 × EMSA binding buffer, 5% glycerol, 2 μg of yeast tRNA, 4–6 μg of protein extract or 600 ng of recombinant human MDH2 protein (Abcam), nuclease-free water, labeled biotinylated RNA probes and/or unlabeled probes. The labeled probe sequences were as follows: CS4: 5′-Biotin-GUGACUAUUUUUGUAAACG-3′, CS5: 5′-Biotin-UUAGCCAUCUUCGGC-3′, CS6: 5′-Biotin-UUAUGUAAAUAGUCAU-3′, CS7: 5′-Biotin-CCUGUGG-UGCACGU-3′. RNA–protein complexes were detected and analyzed using the LightShift Chemiluminescent EMSA Kit (Thermo scientific) according to the manufacturer's suggestions. To assess the interacting specificity of proteins and probes with supershift assays, anti-MDH2 (Abcam) or IgG (Abcam) was added to the samples after incubation with the probes, and incubation was continued for another 10 min at room temperature followed by gel electrophoresis on a native polyacrylamide gel. To further explore the influencing factor, $H_2O_2$ (at a titration of 0.01 to 0.5 μM) and β-Mercaptoethanol (at titration of 0.01 to 0.1 μM) were added into the reactions. RNA EMSA assays using the extracts from seizure mice and control mice were performed with three biological repeats.

### *2.10. Pull down and LC–MS/MS assays*

Pull-down assays were performed using biotinylated oligoribonucleotides and cytoplasmic extracts. Approximately 100 μl of μMACS streptavidin microbeads (Miltenyi Biotec) were used to bind up to 100 pmol of biotinylated oligoribonucleotides according to the manufacturer's recommendations. RNA–protein complexes were isolated by the μMACS separator. The isolated proteins were separated on 10% denatured SDS-PAGE and visualized by Coomassie Blue staining. The band from RNA–protein pull-down assay was excised and submitted for LC–MS/MS assay to identify proteins at the service provided by the BGI (Shenzhen, China). The matched peptides were searched using the Mascot algorithm (www.matrixscience.com).

### *2.11. Hydrogen peroxide assays*

The level of $H_2O_2$ was analyzed using hydrogen peroxide assay kit (S0038, Beyotime Institute of Biotechnology, China) according to the manufacturer's instructions. In brief, the brain tissues were dissolved in the lysis buffer, and then were centrifuged at 12000 rpm for 5 min. The supernatants were collected for the following test. The test tubes containing 100 μl of supernatants and 100 μl of test solutions were placed at room temperature for 20 min and measured instantly with a spectrometer at a wavelength of 560 nm. The concentration of $H_2O_2$ released was calculated according to the standard concentration curve from the standard solution. Three technical repeats were performed with the samples from 5 mice in this study.

### *2.12. Statistical analyses*

All numerical data are expressed as mean ± SEM. Statistical differences among groups were analyzed by one-way ANOVA analysis of variance with a post-hoc test and statistical differences between two groups were determined by the Student's *t*-test. All statistical analyses were performed with SPSS (version 13.0) software. $P < 0.05$ was defined as statistical significance.

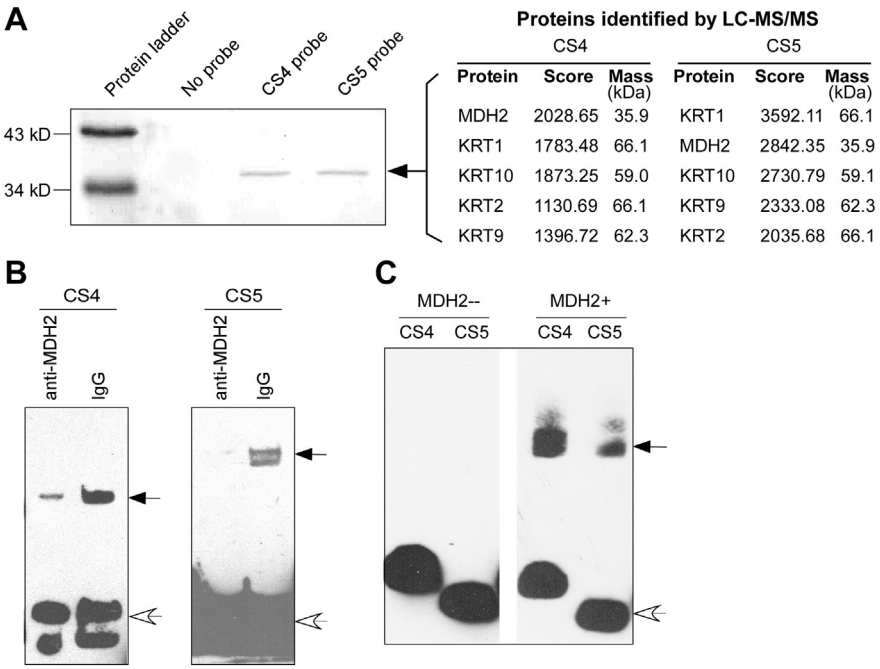


**Fig. 2. MDH2 binds to the conserved regions CS4 and CS5 on the 3′ UTRs of *SCN1A* and *SCN3A*.** (**A**) The CS4 and CS5 binding proteins identified by LC-MS/MS. Proteins pulled down in the absence (No probe) or the presence of the CS4 and CS5 probes were detected by Coomassie staining. The bands (the arrow showed) were excised for protein identification by LC-MS/MS. Five proteins with the highest scores were listed and the molecular weight of MDH2 (35.9 kDa) was similar to that of the pull-down complex in the SDS-PAGE analyses. (**B**) Supershift EMSA assays using anti-MDH2 and IgG, respectively. The shift band was decreased in the reactions using anti-MDH2, compared to the reactions using IgG. Shift probes and free probes were shown by solid arrow and hollow arrow, respectively. (**C**) RNA-EMSA assay using biotin-labeled CS4 and CS5 probes and 200 ng of purified MDH2. The shift bands were observed in the reactions with MDH2 and no retarded band was observed in the reactions without MDH2. Shift probes and free probes were shown by solid arrow and hollow arrow, respectively.

## 3. Results

### *3.1. Identification of the conserved RBP binding sites on the 3′ UTRs of SCN1A and SCN3A genes*

Using the cross-species sequence comparison analysis, we previously identified three conserved regions with length > 15 nts on the 3′ UTRs of human and mouse *SCN1A* and *SCN3A* genes and demonstrated that GAPDH is involved in posttranscriptional regulations of the two genes under seizure condition [15]. Here, we analyzed four conserved regions (named as CS4, CS5, CS6 and CS7, respectively) with a length range from 8 to 15 nts on the 3′ UTRs of human and mouse *SCN1A* and *SCN3A* genes (Fig. 1A). We then used RNA-EMSA assay to identify the potential RNA binding sites using four synthetic oligoribonucleotides containing CS4, CS5, CS6 and CS7, respectively (their sequences shown in Materials and methods). These probes were incubated with cytoplasmic proteins from human HEK293 cells. Shift bands were only observed in the reactions using the CS4 and CS5 probes, but not for the CS6 and CS7 probes (Fig. 1B). To determine whether the binding is specific, we performed competition assays using the unlabeled CS4 and CS5 probes, respectively. Fig. 2C showed that the binding capabilities of the cytoplasmic proteins to the CS4 and CS5 probes were reduced with increased doses of unlabeled probes, suggesting that the CS4 and CS5 are conserved RBP binding sites.

### *3.2. MDH2 functions as an RNA binding protein to bind to the conserved regions of SCN1A and SCN3A 3′ UTRs*

To determine the RNA-binding proteins for the conserved regions, the biotin-labeled RNA probes were used as baits to pull-down interacting proteins from the cytoplasmic extracts of HEK-293 cells. Compared with the negative control (without probes), SDS-PAGE with Coomassie Blue staining showed that ~35-kDa bands was pulled down using the CS4 and CS5 RNA probes, respectively (left in Fig. 2A). The two bands were then excised for LS-MS/MS assay to identify the proteins and several hundreds of proteins were identified as potential RNA-binding proteins (full protein components were provided as required). Fig. 2A (right) showed the five proteins with the highest scores, of them MDH2 might represent a strong candidate due to its molecular weight of 35.9 kDa.

We then performed RNA-EMSA SuperShift assays with the anti-MDH2 to confirm the interaction between MDH2 and the probes. We found that the shift band in the reaction with CS4 and anti-MDH2 was relatively weak compared to the control with IgG, and no shift band in the reaction with CS5 and anti-MDH2 was observed (Fig. 2B). We also performed EMSA assays with the purified recombinant human MDH2 protein to further confirm the interaction. Fig. 2C showed that, after addition of 200-ng MDH2, the strong retarded bands were observed in the reaction using the CS4 and CS5 probes. Thus, these data suggest that MDH2 is an RNA binding protein which binds to the conserved regions of *SCN1A* and *SCN3A* 3′ UTRs.

### *3.3. MDH2 knockdown or inactivation increase gene expression by interacting with the SCN1A 3′ UTR*

To determine whether the binding of MDH2 is involved in regulating gene expression at post-transcriptional level, we used the shRNA-expressing construct for specific knockdown of MDH2 expression. Western blot analyses showed that the MDH2 level in the HEK-293 cells transfected with MDH2-specific shRNA#1 or #2 constructs were respectively 0.2-fold, 0.4-fold of that in the cells transfected with control shRNA constructs (Fig. 3A). We then co-transfected the luciferase constructs containing *SCN1A* 3′ UTR or *SCN3A* 3′ UTR and the shRNA constructs into HEK-293 cells and found that the relative luciferase activities (hRluc/hluc + ) of the constructs containing the *SCN1A* 3′ UTR co-transfected with the MDH2 shRNA#1 or shRNA#2 constructs were respectively 1.8 and 1.5 folds of that of the co-transfected with the control shRNA construct (Fig. 3B), but no altera-

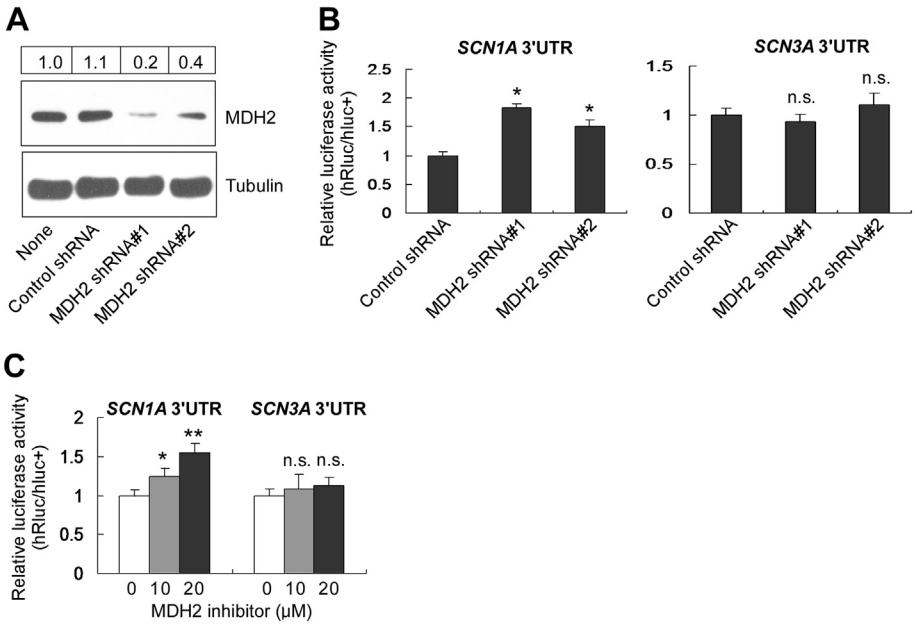


**Fig. 3. Knockdown or inactivation of MDH2 upregulates the reporter gene expression *via SCN1A* 3′ UTR, instead of *SCN3A* 3′ UTR, in HEK-293 cells.** (**A**) Western blot analyses of MDH2 expression in HEK-293 cells transfected with MDH2-specific shRNA or control shRNA. Values at the top show the results of densitometric quantification of MDH2-immunoreactive bands. Tubulin expression was also detected for the loading control. (**B**) The relative activities of the constructs containing *SCN1A* 3′ UTR in the cells transfected with MDH2 shRNA#1 or shRNA#2 were about 1.8 and 1.5 folds of those in the cells transfected with the control shRNA, respectively. No significant difference in the relative activity of the constructs containing *SCN3A* 3′ UTR was observed. The relative activities in the cells transfected with the control shRNA were normalized as "1". $^*P < 0.01$, $n = 10$, n.s. represents no significance. (**C**) The relative activities in the cells transfected with the constructs containing *SCN1A* 3′ UTR, instead of *SCN3A* 3′ UTR, gradually increased following with MDH2 inhibitor at a titration of 0–20 μM. The relative activities in the transfected cells without MDH2 inhibitor were normalized as "1". $^*P < 0.01$, $n = 10$, n.s. represents no significance.

tion in the relative luciferase activity were observed for the constructs containing the *SCN3A* 3′ UTR. To further confirm the effect of MDH2 on the regulation of gene expression *via SCN1A* 3′ UTR, we added MDH2 inhibitor into cultured medium to inhibit MDH2 activity. Fig. 3C showed that the relative activities of the luciferase constructs containing *SCN1A* 3′ UTR in HEK-293 cells treated with 10 and 20 μM of MDH2 inhibitor were respectively ~1.2 and ~1.5 folds of those in the transfected cells without treatment. Similarly, no difference in relative activity was observed for the luciferase constructs containing *SCN1A* 3′ UTR (Fig. 3C). Together, these data suggest that MDH2 plays a role in posttranscriptional regulation of gene expression *via SCN1A* 3′ UTR.

### 3.4. Overexpression of MDH2 downregulates gene expression by affecting mRNA stability

To further investigation the role of MDH2 in posttranscriptional regulation of gene expression, we generate a construct pCMV-MDH2 overexpressing MDH2. Western blots showed that the MDH2 level in the HEK-293 cells transfected with pCMV-MDH2 constructs was ~2.5 folds of that in the cells transfected with the control constructs (Fig. 4A). We then co-transfected the luciferase constructs and the pCMV-MDH2 into HEK-293 cells and found that the relative luciferase activities of the *SCN1A*-3′ UTR-containing constructs co-transfected with the pCMV-MDH2 were only 0.7 fold of that of the co-transfected with the control constructs, but no change in the activities of *SCN3A*-3′ UTR-containing constructs was observed (Fig. 4B). We then detected the effect of MDH2 on the mRNA stability in the transfected HEK-293 cells using actinomycin D (Act.D). After 3- or 6-h Act.D treatment, the remaining relative mRNA levels (*hRluc/hluc* +) of the cells co-transfected with the *SCN1A*-3′ UTR-containing constructs and the MDH2 overexpression constructs were significant lower than those of the cells cotransfected with the *SCN1A*-3′ UTR-containing constructs and the control constructs, and no significant difference in the remaining relative mRNA levels in the transfected cells with *SCN3A*-3′ UTR-containing constructs (Fig. 4C). Therefore, overexpression of MDH2 could downregulate gene expression by affecting mRNA stability.

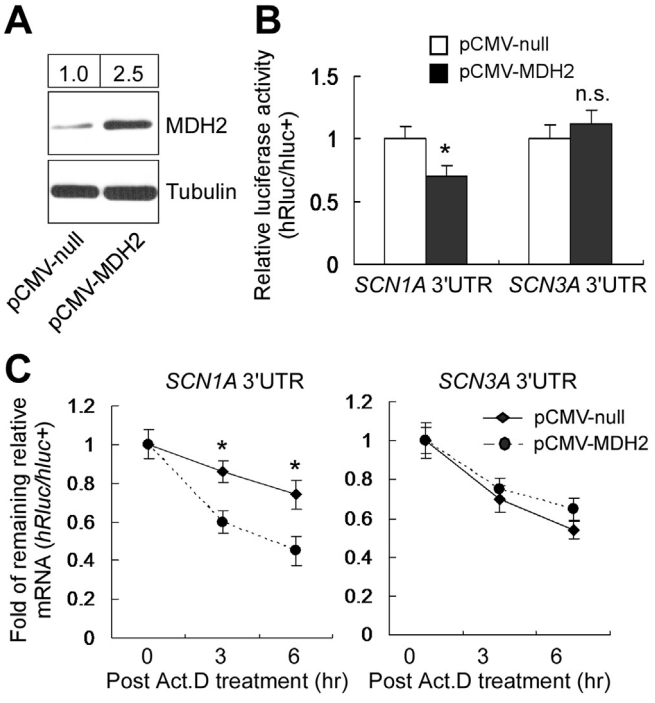


**Fig. 4. Overexpression of MDH2 downregulates the reporter gene expression *via* affecting mRNA stability.** (**A**) Western blot analyses of MDH2 expression in HEK-293 cells transfected with pCMV-MDH2 or pCMV-null. Values at the top show the results of densitometric quantification of MDH2-immunoreactive bands. Tubulin expression was also detected for the loading control. (**B**) The relative activities of the cells cotransfected with the constructs containing *SCN1A* 3′ UTR and pCMV-MDH2 were about 0.7 fold of that in the cells cotransfected with the luciferase construct and pCMV-null. No significant difference in the relative activity was observed for the luciferase constructs containing *SCN3A* 3′ UTR. The relative activities of the cells cotransfected with the constructs containing the luciferase construct and pCMV-null were normalized as "1". $^*P < 0.01$, $n = 3$, n.s. indicates no significance.

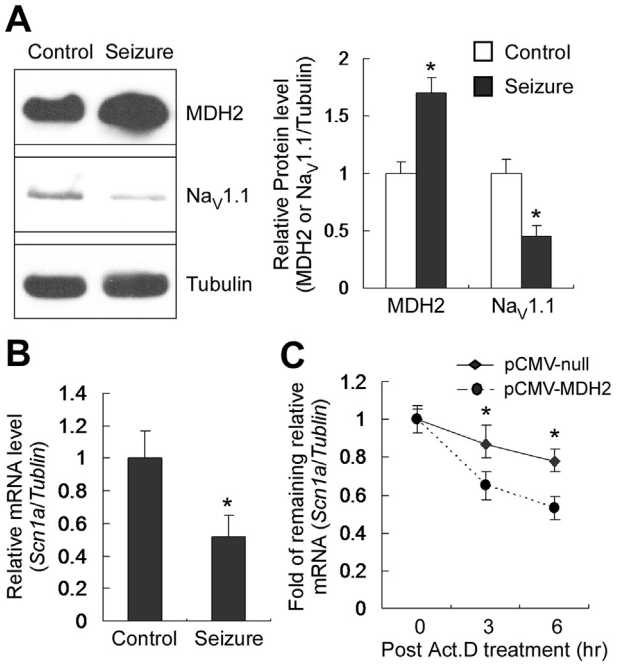


**Fig. 5. Seizure-induced upregulation of MDH2 contributes to decrease *Scn1a* expression *via* affecting mRNA stability.** (**A**) Western blot analyses showing upregulation of MDH2 and downregulation of $Na_V1.1$ in the hippocampus of the seizure mice. The Tubulin expression was also detected for the loading control. The relative average densities of MDH2 or $Na_V1.1$/Tubulin of the control mice were normalized as "1". $n = 3$, $^*P < 0.01$. (**B**) The qRT-PCR showing a decrease of *Scn1a* mRNA levels in the hippocampus of the seizure mice. The relative *Scn1a* mRNA levels (*Scn1a/Tubulin*) in control mice were normalized as "1". $n = 5$, $^*P < 0.01$. (**C**) Overexpression of MDH2 increased the mRNA stability of *Scn1a* gene in mouse N1E-115 cells. The qRT-PCR was used to determine the mRNA levels of *Scn1a* and *Tubulin* genes in N1E-115 cells after 3-h and 6-h treatment with Act.D. The relative *Scn1a* mRNA levels (*Scn1a/Tubulin*) in the cells before treatment were normalized as "1". $^*P < 0.05$, $n = 3$.

### 3.5. Increase of MDH2 expression downregulates Scn1a gene expression in the hippocampus of the seizure mice

Given that MDH2 is involved in the posttranscriptional regulation of *SCN1A* gene expression and abnormal expression of *SCN1A* gene is associated with epileptic seizures [24], we speculate that MDH2-regulated *SCN1A* gene expression may play a role in the development of this disease. Therefore, we generated evoked seizure mice and then detected the protein and mRNA levels of *Mdh2* and *Scn1a* genes. We found that the protein levels of MDH2 and $Na_V1.1$ in the hippocampus of seizure mice were respectively ~1.7 folds and ~0.5 fold of those of normal control mice (Fig. 5A). The qRT-PCR showed that the *Scn1a* mRNA levels in the seizure mice were ~0.5 fold of those in the control mice (Fig. 5B). To determine the relationship between upregulation of MDH2 and downregulation of $Na_V1.1$ in seizure mice, we overexpressed MDH2 in the mouse N1E-115 cells and detected the mRNA stability of *Scn1a* gene. After 3- and 6-h Act.D treatment, the remaining relative mRNA levels (*Scn1a/Tublin*) of the N1E-115 cells transfected with pCMV-MDH2 were significantly lower than that of the cells transfected with pCMV-null (Fig. 5C), suggesting that the increase of MDH2 expression in seizure mice could downregulate *Scn1a* expression *via* affecting the mRNA stability.

### 3.6. Seizure-induced $H_2O_2$ production increases the binding of MDH2 to the conserved elements of Scn1a 3′ UTR

In addition to the increase of MDH2 levels, other factors such as seizure-induced oxidation may also affect the MDH2-mediated regulation of $Na_V1.1$ expression. Therefore, we performed the EMSA analyses using the cytoplasmic extracts with the same quantity of MDH2 between the seizure and control mice (Fig. 6A). The results showed that the density of retarded bands using the extracts from seizure mice increased ~5 folds (for CS4 probes) and ~3 folds (for CS5 probes) of those using the extracts from control mice (Fig. 6A), suggesting that seizure could promote the binding of MDH2 to the conserved elements. We then assayed $H_2O_2$ levels of the hippocampus and found that the

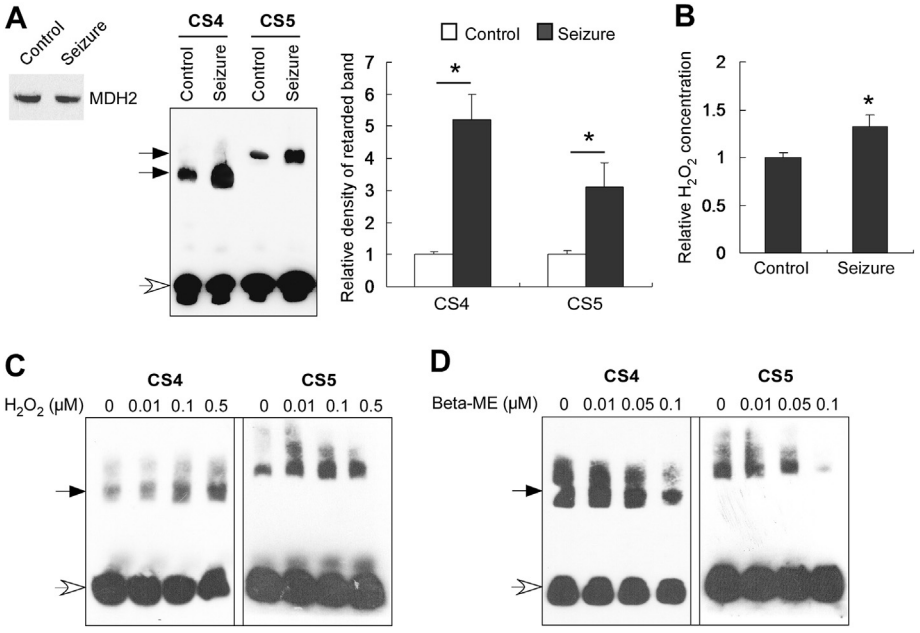


**Fig. 6. Seizure-induced increase in $H_2O_2$ enhances the binding of MDH2 to the CS4 and CS5 elements.** (**A**) RNA-EMSA showing that the binding of MDH2 to the CS4 and CS5 elements increased using the cytoplasmic extracts from seizure mice compared to control mice. Western blot (left figure) represented the same usage of MDH2 between the seizure mice and the control mice. The densities of the retarded bands using the cytoplasmic extracts from the control mice were normalized as "1". $^*P < 0.01$, $n = 3$. (**B**) $H_2O_2$ levels in the hippocampus of seizure mice increased compared to control mice. The levels of $H_2O_2$ in hippocampus of control mice were normalized as "1". $n = 5$, $^*P < 0.01$. (**C**) RNA-EMSA showing that the retarded probes in the assays gradually increased following with increasing the usage of $H_2O_2$. (**D**) RNA-EMSA showing that the retarded probes in the assays gradually decreased following with increasing the usage of β-ME.

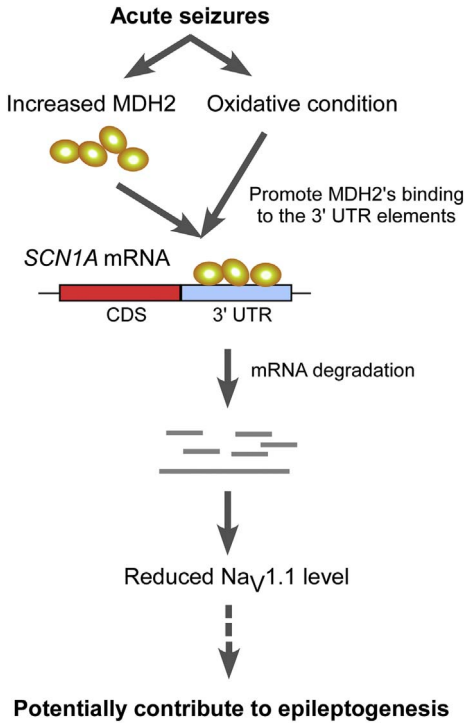


**Fig. 7.** Schematic illustration of the potential role of MDH2 in epileptogenesis *via* posttranscriptional downregulation of $Na_V1.1$ expression.

$H_2O_2$ concentrations in the hippocampus of the seizure mice were ~1.3 folds of that of the control mice (Fig. 6B). To determine the role of $H_2O_2$ on the interaction between MDH2 and the conserved motifs, we performed EMSA using purified MDH2 and found that the binding capability of the MDH2 to the CS4 and CS5 gradually increased following a titration of $H_2O_2$ at 0–0.5 μM (Fig. 6C). On the contrast, the binding capability of the MDH2 to the CS4 and CS5 gradually decreased following a titration of β-Mercaptoethanol at 0.01–0.1 μM (Fig. 6D). Together, these data suggest that seizure-induced $H_2O_2$ production increases the binding of MDH2 to the *Scn1a* 3′-UTR motifs, which then downregulates *Scn1a* expression.

## 4. Discussion

In this study, we report for the first time that MDH2, a critical metabolic enzyme in TCA cycle, functions as an RNA binding protein to alter *SCN1A* gene expression at post-transcriptional level. We demonstrate that MDH2 binds to the conserved elements of *SCN1A* 3′ UTR and negatively regulates this gene expression, which contribute to the downregulation of mouse *Scn1a* expression under seizure-induced oxidative condition (Fig. 7). Due to the strong relationship of $Na_V1.1$ deficiency with epilepsy [2,24], thus this work provides a link between the MDH2-induced downregulation of *SCN1A* expression and seizures.

Using the sequence comparison and LS-MS/MS analyses similar to one of our recent studies [15], we identified that MDH2 could bind to two of four conserved regions with a length range from 8 to 15 nts on the 3′ UTRs of human and mouse *SCN1A* and *SCN3A* genes. It is known that MDH2 is a nuclear gene encoding mitochondrial protein which catalyzes the reversible oxidation of malate to oxaloacetate in the citric acid cycle, *i.e.*, this protein is synthesized in the cytoplasm and then is transported into the mitochondria. Given that MDH2 is an RNA binding protein that interacts with the *SCN1A* 3′ UTR elements and a previous report that many metabolic enzymes including MDH2 are suggested as potential RNA binding proteins [12], we speculate that this protein might play multiple roles in cytoplasm.

We previously showed that another metabolic enzyme GAPDH binds to a conserved region in the 3′ UTRs of human and mouse *SCN1A* and *SCN3A* genes that posttranscriptionally regulates the expressions of the two genes [15]. However, the present study found that MDH2s binding to the conserved 3′-UTR motifs downregulated gene expression by affecting mRNA stability *via SCN1A* 3′ UTR, instead of *SCN3A* 3′ UTR, although these motifs are presented in 3′ UTRs of both *SCN1A* and *SCN3A* genes. This phenomenon might be resulted from the distinct second structures of the two genes and/or their recruited interacting co-factors. Future studies are needed to explore the underlying mechanism.

Our data showed that MDH2 was upregulated and $Na_V1.1$ was downregulated in the hippocampus of acute seizure mice. We further showed that overexpression of MDH2 in mouse cell line decreased the *Scn1a* mRNA stability, suggesting a causal link between the change of MDH2 and $Na_V1.1$. In line with our previous report that GAPDH contributes to downregulate *Scn1a* expression under seizure condition [15], we speculate that both MDH2 and GAPDH share a combined role in the regulation of *Scn1a* expression. Given that the two proteins are metabolic enzymes and epileptic seizures are associated with metabolism [25], thus this study provide a direct link between seizure and metabolism.

The present study further showed that seizure-induced oxidation promotes the binding of MDH2 to the 3′-UTR elements and the reducing condition decreases these bindings, which can be explained by the MDH2 modifications such as phosphorylation under redox conditions, similar to that of GAPDH [15,26,27]. Accumulating evidences suggest that oxidative stress is a consequence of the first onset of seizure, which then potentially contribute to epileptogenesis [28,29], therefore, it is possible that MDH2-mediated downregulation of *Scn1a* expression under seizure-induced oxidation condition might be involved epileptogenesis.

Mutations in the *MDH2* gene are associated with several cancers and its protein product may be a potential target for cancer treatment [30,31]. According to this idea and our findings, we propose that MDH2 may be an effective therapeutic target for seizure control.

## Transparency Document

The http://dx.doi.org/10.1016/j.bbadis.2017.04.018 associated with this article can be found in the online version.

## Conflict of interest statement

All authors declare that they have no conflict of interest.

## Acknowledgements

This work is supported by The National Natural Science Foundation of China (81371436, 81671112 and 81471149), The Innovative Academic Teams of Guangzhou Education System (1201610025), and partially supported by the Collaborative Innovation Center for Neurogenetics and Channelopathies. We are grateful to the He Shanheng Charity Foundation for contributing to the development of this institute.

## References

[1] H. Meng, H.Q. Xu, L. Yu, G.W. Lin, N. He, T. Su, Y.W. Shi, B. Li, J. Wang, X.R. Liu, B. Tang, Y.S. Long, Y.H. Yi, W.P. Liao, The SCN1A mutation database: updating information and analysis of the relationships among genotype, functional alteration, and phenotype, Hum. Mutat. 36 (2015) 573–580.

[2] M.H. Meisler, J.A. Kearney, Sodium channel mutations in epilepsy and other neurological disorders, J. Clin. Invest. 115 (2005) 2010–2017.

[3] T. Nakayama, I. Ogiwara, K. Ito, M. Kaneda, E. Mazaki, H. Osaka, H. Ohtani, Y. Inoue, T. Fujiwara, M. Uematsu, K. Haginoya, S. Tsuchiya, K. Yamakawa, Deletions of SCN1A 5′ genomic region with promoter activity in Dravet syndrome, Hum. Mutat. 31 (2010) 820–829.

[4] T. Zeng, Z.F. Dong, S.J. Liu, R.P. Wan, L.J. Tang, T. Liu, Q.H. Zhao, Y.W. Shi, Y.H. Yi, W.P. Liao, Y.S. Long, A novel variant in the 3′ UTR of human SCN1A gene

from a patient with Dravet syndrome decreases mRNA stability mediated by GAPDH's binding, Hum. Genet. 133 (2014) 801–811.
[5] Q.W. Gao, L.D. Hua, J. Wang, C.X. Fan, W.Y. Deng, B. Li, W.J. Bian, C.X. Shao, N. He, P. Zhou, W.P. Liao, Y.W. Shi, A point mutation in SCN1A 5′ genomic region decreases the promoter activity and is associated with mild epilepsy and seizure aggravation induced by antiepileptic drug, Mol. Neurobiol. (2016).
[6] F.H. Yu, M. Mantegazza, R.E. Westenbroek, C.A. Robbins, F. Kalume, K.A. Burton, W.J. Spain, G.S. McKnight, T. Scheuer, W.A. Catterall, Reduced sodium current in GABAergic interneurons in a mouse model of severe myoclonic epilepsy in infancy, Nat. Neurosci. 9 (2006) 1142–1149.
[7] C. Cheadle, J. Fan, Y.S. Cho-Chung, T. Werner, J. Ray, L. Do, M. Gorospe, K.G. Becker, Control of gene expression during T cell activation: alternate regulation of mRNA transcription and mRNA stability, BMC Genomics 6 (2005) 75.
[8] W. Filipowicz, S.N. Bhattacharyya, N. Sonenberg, Mechanisms of post-transcriptional regulation by microRNAs: are the answers in sight? Nat. Rev. Genet. 9 (2008) 102–114.
[9] C. Andreassi, A. Riccio, To localize or not to localize: mRNA fate is in 3'UTR ends, Trends Cell Biol. 19 (2009) 465–474.
[10] K.A. Spriggs, M. Bushell, A.E. Willis, Translational regulation of gene expression during conditions of cell stress, Mol. Cell 40 (2010) 228–237.
[11] S.S. Peng, C.Y. Chen, N. Xu, A.B. Shyu, RNA stabilization by the AU-rich element binding protein, HuR, an ELAV protein, EMBO J. 17 (1998) 3461–3470.
[12] A. Castello, B. Fischer, K. Eichelbaum, R. Horos, B.M. Beckmann, C. Strein, N.E. Davey, D.T. Humphreys, T. Preiss, L.M. Steinmetz, J. Krijgsveld, M.W. Hentze, Insights into RNA biology from an atlas of mammalian mRNA-binding proteins, Cell 149 (2012) 1393–1406.
[13] K.S. Khabar, Post-transcriptional control of cytokine gene expression in health and disease, J. Interferon Cytokine Res. 34 (2014) 215–219.
[14] A. Castello, M.W. Hentze, T. Preiss, Metabolic enzymes enjoying new partnerships as RNA-binding proteins, Trends Endocrinol. Metab. 26 (2015) 746–757.
[15] G.W. Lin, P. Lu, T. Zeng, H.L. Tang, Y.H. Chen, S.J. Liu, M.M. Gao, Q.H. Zhao, Y.H. Yi, Y.S. Long, GAPDH-mediated posttranscriptional regulations of sodium channel Scn1a and Scn3a genes under seizure and ketogenic diet conditions, Neuropharmacology 113 (2017) 480–489.
[16] J.S. Muller, M. Giunta, R. Horvath, Exosomal protein deficiencies: how abnormal RNA metabolism results in childhood-onset neurological diseases, J. Neuromuscul. Dis. 2 (2015) S31–S37.
[17] T. Zeng, Z.F. Dong, S.J. Liu, R.P. Wan, L.J. Tang, T. Liu, Q.H. Zhao, Y.W. Shi, Y.H. Yi, W.P. Liao, Y.S. Long, A novel variant in the 3′ UTR of human SCN1A gene from a patient with Dravet syndrome decreases mRNA stability mediated by GAPDH's binding, Hum. Genet. 133 (2015) 801–811.
[18] G.F. Deng, J.M. Qin, X.S. Sun, Z.Y. Kuang, T. Su, Q.H. Zhao, Y.W. Shi, X.R. Liu, M.J. Yu, Y.H. Yi, W.P. Liao, Y.S. Long, Promoter analysis of mouse Scn3a gene and regulation of the promoter activity by GC box and CpG methylation, J. Mol. Neurosci. 44 (2011) 115–121.
[19] Y.S. Long, Q.H. Zhao, T. Su, Y.L. Cai, Y. Zeng, Y.W. Shi, Y.H. Yi, H.H. Chang, W.P. Liao, Identification of the promoter region and the 5′-untranslated exons of the human voltage-gated sodium channel Nav1.1 gene (SCN1A) and enhancement of gene expression by the 5′-untranslated exons, J. Neurosci. Res. 86 (2008) 3375–3381.
[20] M. Penkowa, S. Florit, M. Giralt, A. Quintana, A. Molinero, J. Carrasco, J. Hidalgo, Metallothionein reduces central nervous system inflammation, neurodegeneration, and cell death following kainic acid-induced epileptic seizures, J. Neurosci. Res. 79 (2005) 522–534.
[21] H.J. Li, R.P. Wan, L.J. Tang, S.J. Liu, Q.H. Zhao, M.M. Gao, Y.H. Yi, W.P. Liao, X.F. Sun, Y.S. Long, Alteration of Scn3a expression is mediated via CpG methylation and MBD2 in mouse hippocampus during postnatal development and seizure condition, Biochim. Biophys. Acta 1849 (2015) 1–9.
[22] N.N. Tan, H.L. Tang, G.W. Lin, Y.H. Chen, P. Lu, H.J. Li, M.M. Gao, Q.H. Zhao, Y.H. Yi, W.P. Liao, Y.S. Long, Epigenetic downregulation of Scn3a expression by valproate: a possible role in its anticonvulsant activity, Mol. Neurobiol. (2016).
[23] E.V. Gazina, K.L. Richards, M.B. Mokhtar, E.A. Thomas, C.A. Reid, S. Petrou, Differential expression of exon 5 splice variants of sodium channel alpha subunit mRNAs in the developing mouse brain, Neuroscience 166 (2010) 195–200.
[24] F.H. Yu, M. Mantegazza, R.E. Westenbroek, C.A. Robbins, F. Kalume, K.A. Burton, W.J. Spain, G.S. McKnight, T. Scheuer, W.A. Catterall, Reduced sodium current in GABAergic interneurons in a mouse model of severe myoclonic epilepsy in infancy, Nat. Neurosci. 9 (2006) 1142–1149.
[25] S. Rahman, E.J. Footitt, S. Varadkar, P.T. Clayton, Inborn errors of metabolism causing epilepsy, Dev. Med. Child Neurol. 55 (2013) 23–36.
[26] L.P. Liang, M. Patel, Seizure-induced changes in mitochondrial redox status, Free Radic. Biol. Med. 40 (2006) 316–322.
[27] A. Pierce, H. Mirzaei, F. Muller, E. De Waal, A.B. Taylor, S. Leonard, H. Van Remmen, F. Regnier, A. Richardson, A. Chaudhuri, GAPDH is conformationally and functionally altered in association with oxidative stress in mouse models of amyotrophic lateral sclerosis, J. Mol. Biol. 382 (2008) 1195–1210.
[28] M.N. Patel, Oxidative stress, mitochondrial dysfunction, and epilepsy, Free Radic. Res. 36 (2002) 1139–1146.
[29] S. Puttachary, S. Sharma, S. Stark, T. Thippeswamy, Seizure-induced oxidative stress in temporal lobe epilepsy, Biomed. Res. Int. 2015 (2015) 745613.
[30] A. Cascon, I. Comino-Mendez, M. Curras-Freixes, A.A. de Cubas, L. Contreras, S. Richter, M. Peitzsch, V. Mancikova, L. Inglada-Perez, A. Perez-Barrios, M. Calatayud, S. Azriel, R. Villar-Vicente, J. Aller, F. Setien, S. Moran, J.F. Garcia, A. Rio-Machin, R. Leton, A. Gomez-Grana, M. Apellaniz-Ruiz, G. Roncador, M. Esteller, C. Rodriguez-Antona, J. Satrustegui, G. Eisenhofer, M. Urioste, M. Robledo, Whole-exome sequencing identifies MDH2 as a new familial paraganglioma gene, J. Natl. Cancer Inst. 107 (2015).
[31] Y.W. Lo, S.T. Lin, S.J. Chang, C.H. Chan, K.W. Lyu, J.F. Chang, E.W. May, D.Y. Lin, H.C. Chou, H.L. Chan, Mitochondrial proteomics with siRNA knockdown to reveal ACAT1 and MDH2 in the development of doxorubicin-resistant uterine cancer, J. Cell. Mol. Med. 19 (2015) 744–759.